Iraqi Journal of Nanotechnology

synthesis and application

Controlling the Tube Diameter of SWCNTs Using High Melting Point Promotors

Haider Hassan Almkhelfe

Midland Refineries Company MRC, Ministry of Oil, Baghdad, Iraq
Email: halwan@ksu.edu

Keywords:

Single-Walled Carbon
Nanotubes;
Ru as promoter;
Chirality Control

Abstract

A particular control of the diameter of Single Walled-Carbon Nanotube (SWCNT) using Chemical vapor Deposition (CVD) system will enable many promising applications in different fields. Here we demonstrate the growth of SWCNT with good control of diameter (1.5 nm ± 0.7) using a high melting temperature metal (Ru) as a catalyst promotor with the main catalyst Co at 850˚C via CVD. We hypothesis that using high melting temperature metal as a promotor, like Ru can limit the mobility/change in the shape of the formed metal nanoparticles and eventually decrease the effects of Ostwald ripening (OR). FTS-GP is used as a carbon precursor. The results have been verified by high-resolution transmission electron microscopy (HR-TEM), atomic force microscopy (AFM) and multi-excitation Raman.

Introduction

Controlling the diameter of single walled-Carbon nanotubes (SWCNTs), considered one of the challenging aspects that researchers have faced in the area of synthesizing SWNTs. Electronic and optical properties of SWCNTs highly influence their geometric orientations, like chirality index (n,m). [1] Generally, SWNT is classified either as metallic (m-SWNTs) or semiconductors (s-SWNTs) based on the tube diameter size where the tube diameter inverses proportionally with the band gap [2], which consider as the tunable electronic property of SWNTs. A big band gap tubes (s-SWNTs), preferable in the field of electronics since those big band gaps will serve as channels in the field-effective transistors (FETs) [3]. An extensive theoretical and experimental studies have concluded that catalyst particles size one of the key factors that formulate the SWCNT diameter size. [4]-[6]

The typical growth of SWNTs carpet is a coexist of both metallic and semiconductor nanotubes (wide range of SWNTs diameter) which limit their application. In order to increase the participation of SWCNTs in electronic devices, controlling the tube diameter of SWCNT is required. Recently, attempts have been focused on separating the semiconducting from metallic tubes by using physical separation like dielectrophoresis and density gradient centrifugation, also, chemical separation methods, for instance, adsorption of bromine and diazotization [7]-[10]. However, those approaches frequently lead to short and defected tube or highly contaminated which may affect the performance of the nanotube and subsequently the device performance [3]. Also, those techniques do not always offer a high selectivity besides those separation methods are non-scalable [11]. A chemical vapor deposition (CVD) method one of the processes that consider as a sufficient tool to improve the SWNTs diameter. Catalyst particle size is the main problem solver to obtain smaller diameter [12],[13], however, researchers have shown that other parameters can also be able to control the tube diameter size, such as

manipulating the growth temperature which effects the activation energy of the carbon precursor [14] or by changing the concentration of the precursor, Tian et al. was able to control the SWNTs diameter from 1.2-1.9 nm by changing the concentration of carbon dioxide [15]. An extensive survey study using density functional theory (DFT) was used to investigate different parameters that can affect the SWNTs diameter. The study concluded the catalyst particle size is one of the main parameters responsible for nucleating the SWNTs with a specific diameter [16]. Due to aggregation (Ostwald ripening), that can happen at high temperatures causing a wide range in particle size distributions. One way to overcome this problem is by leaving sufficient space between catalyst particles prevent them from aggregating and allow them to form smaller particle size [13],[16]-[19]. However, the growth results base on the catalyst particle spacing is not with sufficient dens (carpet growth) which is a very important aspect in so many applications [20]. Mattevi et al. suggested that the supporting layer AlOy plays an important rule by reducing the mobility of the iron catalyst and prevent the Ostwald ripening effects due to the strong interaction with the support at high growth temperature [21], while Kim et al. proposed the growth termination step start when the iron particles start diffuses through the alumina support [22]. Other research groups have initiate what is called "cloning growth" which is a metal-free growth system to eliminate all the termination and contamination that can be caused by metal particles [23]-[25]. This type of growth shows a good control of SWNTs chirality, and since this growth type is based on open-ends SWNTs seed, the density of the resulted growth is limited by a few tubes and they are off-substrate.

In this work, we show good control of SWNTs diameter and hence a chirality by using FTS-GP as carbon precursor and by using high melting point metals (Ru) as catalyst promoters using atmospheric pressure chemical vapor deposition (CVD). The growth results show a well-defined selective growth of narrow diameter distribution of SWNTs on cobalt and iron as main catalysts at their perspective growth temperature.

Experimental Work

The morphologies and microstructures of the grown SWCNTs were studied by field emission scanning electron microscopy (FESEM) using FEI Versa 3D dual beam with multiple detectors and transmission electron microscopy (TEM). For TEM imaging, a small amount of SWCNT carpet sample was mechanically exfoliated from the substrate and dispersed in ethanol via sonication. A drop of the homogeneous suspension was deposited on a lacey carbon TEM grid and examined by TEM using FEI Tecnai F20 XT operating at 200 kv. The structure and quality of SWCNTs were characterized by Raman spectroscopy using a multi-laser wavelength of 488, 514, 633, and 785nm. Raman spectra were collected at multiple spots from the samples using a Renishaw inVia Raman microscope. Atomic force microscopy (AFM) was used for mapping the catalyst surface topography prior to and after SWCNT growth. The catalyst film with a nominal thickness of 0.5 nm Co or Fe, 0.1 nm Ru (as catalyst promotor), and 30 nm supporting layer (AlxOy) were deposited on Si (100) wafers with a native oxide layer by ion beam sputtering (IBS/e, South Bay Technology). The metal targets were etched to remove the native oxide layer prior to deposition. All films were deposited at 10-4 Torr chamber pressure using a voltage of 8 kV and a current of 6 mA under Ar flow, without exposing the films to air between depositions. The carbon feedstock (FTS-GP), supplied by Matheson Inc., had the following composition: H_2 (40%), CH_4 (30%), C_2H_6 (8%), C_2H_4 (6%), CO (5%), C_3H_8 (5%), N_2 (4%), and C_3H_6 (2%) as a typical product mixture obtained from FTS process.[26],[27] SWCNT growth was carried out at atmospheric pressure using the EasyTube 101 CVD system (CVD Equipment Corporation), equipped with several important features including LabView-based process control software, static mixer for optimum gas mixing, and control system for precise temperature control. A typical growth run involved heating the catalyst sample to the desired temperature (850°C) at a rate of 45 °C/min in flowing Ar. At the growth temperature, the catalyst was exposed to a copious amount of H_2 in combination with Ar for 2 min to reduce the catalyst; the respective flow rates were 250 standard cubic centimeters per minute (sccm) H_2 and 250 sccm Ar. Thereafter, SWCNT growth under optimum conditions on a Co/Ru catalyst was initiated by introducing 10 sccm FTS-GP and 100 sccm Ar at various times. At the end of the growth run, the samples were rapidly cooled in H_2, followed by slow cooling to room temperature in 700 sccm Ar.

Results and discussion

A high melting temperature metal Ru was used as Co catalyst promotor to control the size of SWCNT growing by atmospheric pressure chemical vapor deposition (CVD). The dispersion without agglomeration during CVD annealing achieved with 0.1 nm of Ru used as promotors with 0.5 nm of Co. In the absence of Ru, Co catalyst experience sever Ostwald ripening (OR) as particles larger than 5 nm are formed, Figure 1, shows the atomic force microscopy of Co catalyst (a) and Co/Ru (b) after annealing in a hydrogen environment at 850˚C. OR formation rate is a temperature-dependent, [28] as the growth temperature increase nanoparticles have more tendency to agglomerate via OR or sintering as an attempts to minimize their surface energy, and since the tube diameter of SWCNT is highly effected by catalyst particles size therefore an extra work needs to be invested in this area. Experiments and theoretical models have concluded that OR and subsurface diffusion are the main two critical factors affecting the size of catalyst particles, and subsequently the tube diameter in SWCNT. [29] Pretreatment of the catalyst support by ion beam bombardment and thermal annealing was found to be an effective approach to minimize the effect of OR and obtain ultra-narrow tube diameter in SWCNT. [30] Inhibiting the Ostwald ripping was also reported by introducing H_2O along with H_2 during annealing to reduce the diffusion rates of catalyst atoms. [31] The nanoparticles tried to minimize their surface energy by making big clusters at high temperatures.
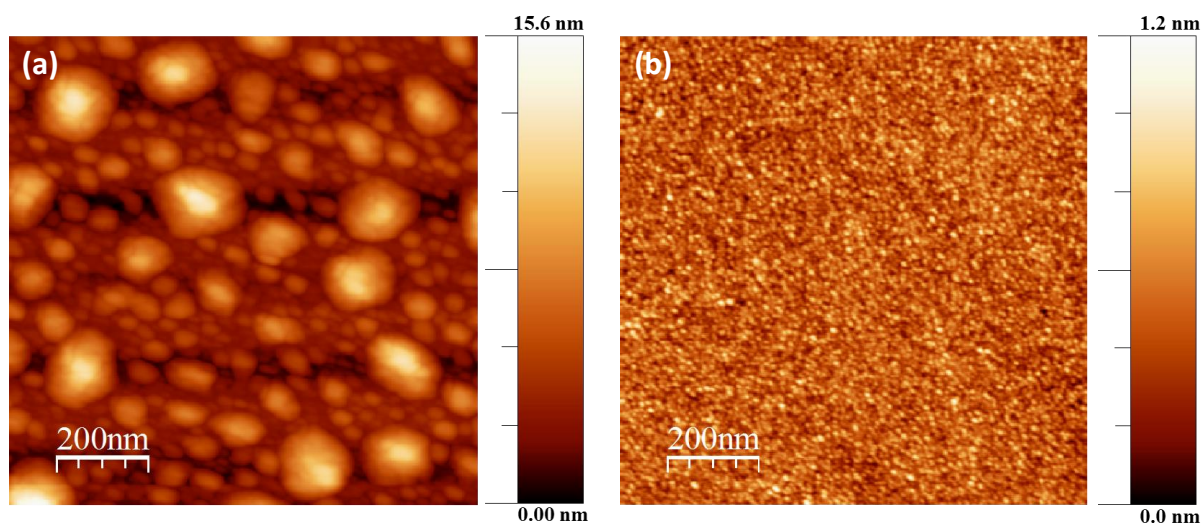

Figure 1. AFM microscopy after H2-annealing at 850˚C for 5 min for Co catalyst (a) and Co/Ru catalyst (b).

Thermal dewetting of the deposited metal films into finely/homogeneously nanoparticles is highly dependent on the melting point of that metal and the porosity of the under layer.[30] We hypothesis that using high melting temperature metal as a promotor, like Ru can limit the mobility of the formed Co particles and eventually decrease the effects of OR. The same observation has been reported by using platinum (Pt) with Co as a bimetallic catalyst, [32] where Pt plays a crucial role to stabilize the Co catalyst and obtain a narrower tube diameter. Also, using Ru with Fe as a bimetallic catalyst can affordably grow SWCNT with the narrow diameter and chirality distribution.[6]
 The TEM images shown in Figure 2 illustrate the morphology and tube diameter growing using AlOx supported Co-Ru (a,b) and Co (d,e). The difference in tube diameter is very obvious and further supporting the role of the high melting temperature promotor (Ru) to control the average dimeter size from 2.5 to 1.5 nm as shown in Figure 1 (c,f). Suggesting that introducing catalyst promotors can significantly impact the reaction pathway and alter the SWCNT diameter size. In comparison with adjusting the reaction parameters, Kiang et al. show that changing the reaction environment may only fine-tune the distribution.[33] The effects of Ru was investigated on Fe catalyst using TEM microscopy at 750ºC with the same carbon precursor (FTS-GP). The average diameter of the grown SWCNT from Fe-Ru was smaller (1.9 nm) compared with Fe catalyst (3.1 nm). Dai et al. explained the effect of Ru in bimetallic catalyst Fe/Ru to form smaller tube dimeter to their alloying structure and strong Fe-Ru interaction to afford smaller catalyst nanoparticles stable against high temperature sintering.6
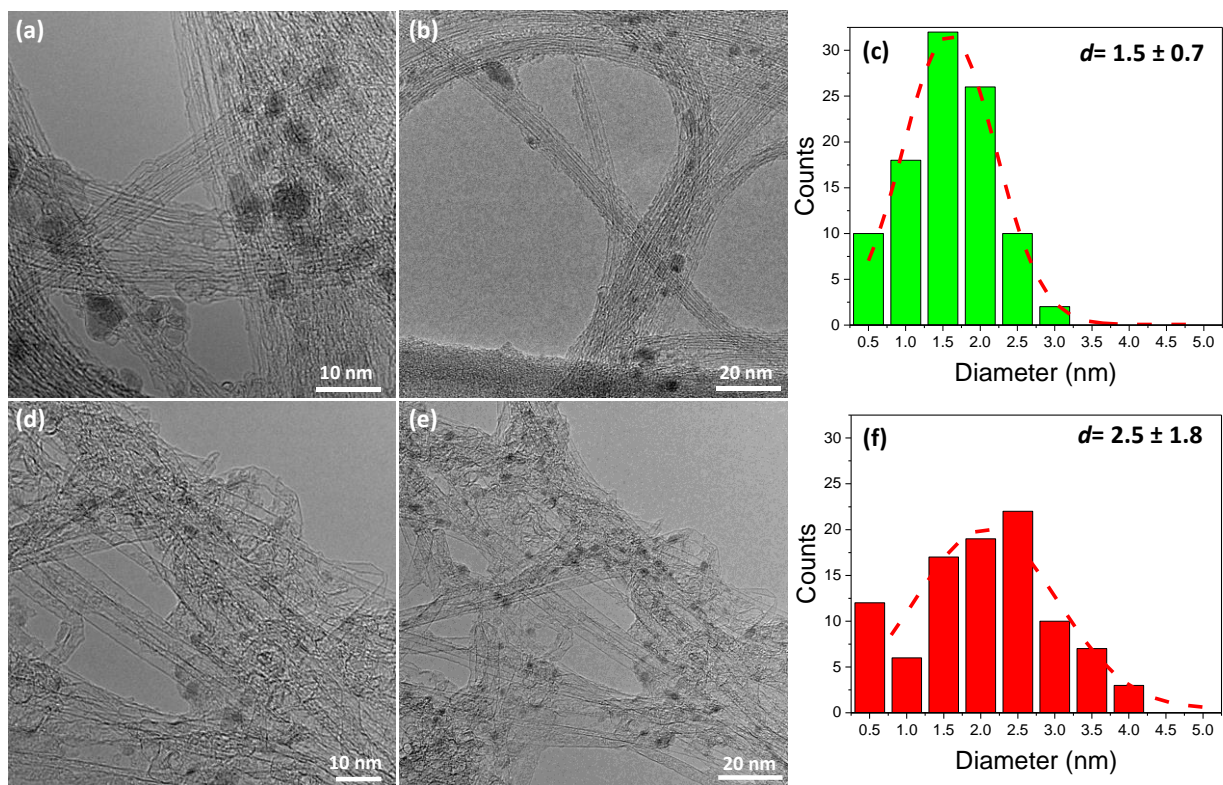
Figure 2. HR-TEM images of SWCNT growing via CVD and FTS-GP as carbon precursors at 850°C, using Co/Ru supported on AlOx (a,b) with diameter distribution (c), and using Co supported AlOx (d,e) with diameter distribution (f).

The effects of Ru were also studied on Co and Fe catalysts by using Raman scattering techniques with laser excitation wavelength in the range from 488 to 785 nm. Various Raman peaks were observed and identified with a low-frequency radial breathing mode (RBM), which is the characteristic signature of SWCNT. Figure 3 (a,b) shows the effect of Ru on Fe catalyst at its optimum temperature (750°C), where the peaks shift toward 300 cm-1 are clear. Using a laser with wavelength 488 and 514 nm introduces a new peak of Fe-Ru catalyst at Raman shift 275cm-1 while exciting the SWCNT with 633 nm, two highly intense peaks (280, 300 cm-1) are observed. Exciting the SWCNT grown by Fe-Ru catalyst with a wavelength 785 nm increase the intensity of the peak 260 cm-1 that already observed with SWCNT grown by Fe catalyst.
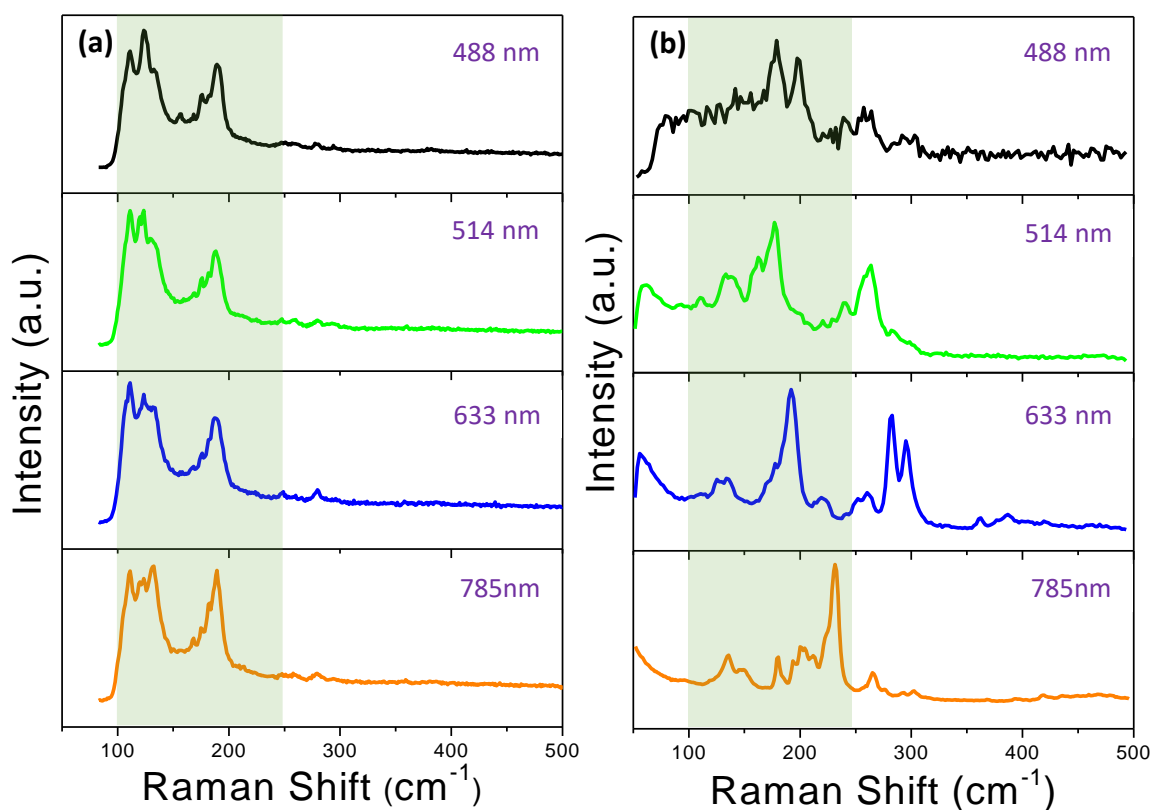
Figure 3. Multi-excitation Raman spectra of SWCNT synthesis as 750˚C of Fe catalyst (a) and Fe-Ru catalyst (b).

Figure 4 Raman mapping of SWCNT grown by Co-Ru and Co at its optimum temperature (850ºC). Clear differences are observed between the two samples. Although the growth of SWCNT has been carried at a much higher temperature compare with Fe catalyst, the role of Ru still effective. Multi-new peaks have been observed at high Raman shift with Co-Ru and they are in good agreement with TEM microscopy results. The laser with a wavelength of 514 nm shows the significance of using Co-Ru as an active catalyst for smaller SWCNT diameter two peaks were identified at 250 and 265 cm-1. Also, exciting the SWCNT grown by Co-Ru with 785 nm increase the intensity of the peak observed at 275 cm-1, indicating an enhancement in yield of smaller diameter size.
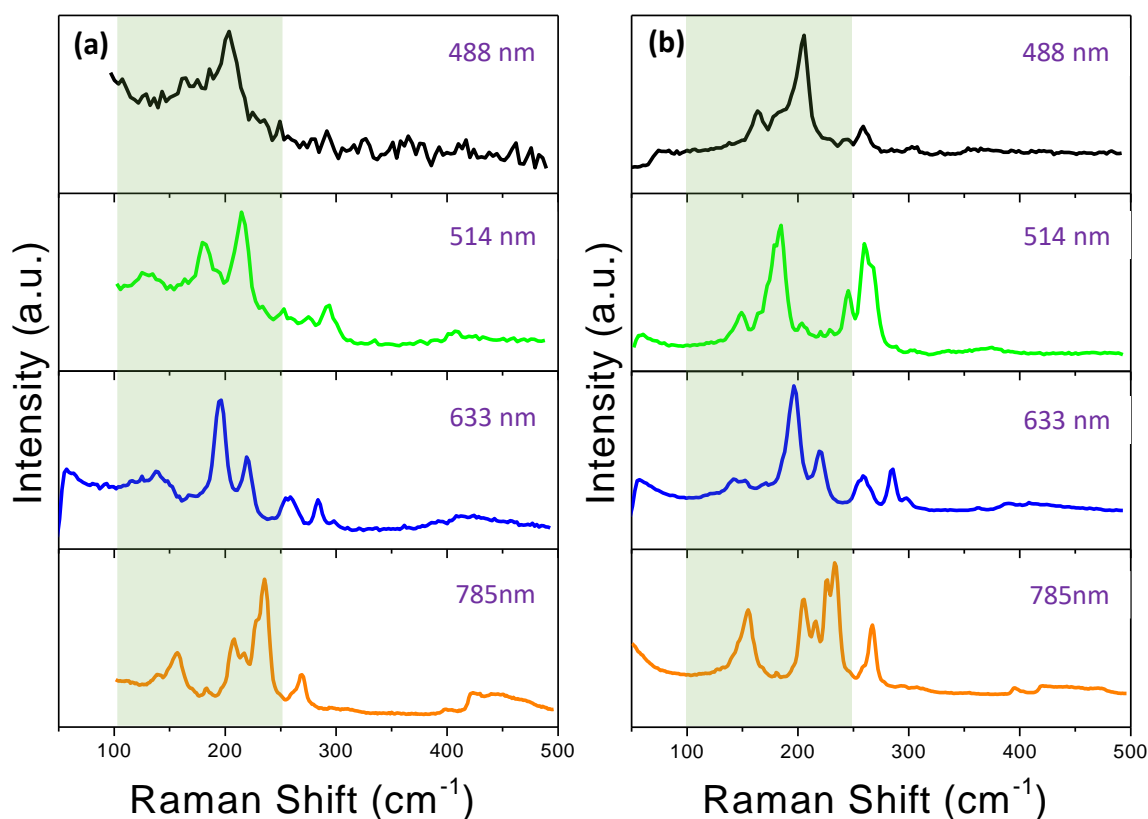
Figure 4. Figure 3. Multi-excitation Raman spectra of SWCNT synthesis as 850˚C of Co catalyst (a) and Co-Ru catalyst (b).

High melting point metal tungsten (W) used with Co as a bimetallic catalyst for synthesizing SWCNT,[34] the growth results show a high selectivity toward a specific chirality (12,6). Balbuena et al. have carried a modeling simulation to predict the parameters that can influence the chirality of SWCNT.[35] Changing the catalyst shape during growth is the main factor that can impact the chirality and tube diameter size, also found by strengthening the metal-substrate interaction a more stable particle shape can be obtained. So we believe using the promotor Ru with Fe and Co catalyst controls the dewetting of the catalyst nanoparticles to offer a more stable structure shape during SWCNT growth. Using the catalyst promotor (Ru) with Co and Fe also ensures the high quality of the as-grown SWCNTs based on the intensity ratio of defect-induced D-band to tangential G-band.

Resonant Raman scattering was used to carry a comprehensive study of the chiral-index assignment of SWCANT assuming the nanotube is a homogeneous cylinder that the frequency of the RBM is linear with the inverse diameter according to empirical equation (ωRBM= 1/d).[36] The SWCNT diameter (dt) can be calculated using the following formula: dt = 223.5/(ωRBM – 12.5) Where ωRBM is the Raman shift of RBM of SWCNT in cm-1.

Conclusion

SWCNT diameter size control is a prerequisite for particular applications in electronic and optoelectronic devices. We have demonstrated the role of high melting temperature metal (Ru) as a catalyst promotors with Fe and Co using ion beam sputtering for catalyst preparation. FTS-GP used as carbon precursor at 750ºC for Fe catalyst and 850ºC for Co. Introducing 0.1 nm of Ru into Fe or Co catalyst strongly influence the diameter size distribution of SWCNT. The average diameter size of SWCNT reduced from 2.5 nm (using Co catalyst) to 1.5 nm when Ru is used as the promoter. While using Ru with Fe catalyst reduces the diameter size of the grown SWCNT from 3.1 to 1.9 nm. Further, Ru has also enhanced the quality of the grown SWCNT by increasing the intensity of the G-band.

References

1. Chiashi, S.; Kono, K.; Matsumoto, D.; Shitaba, J.; Homma, N.; Beniya, A.; Yamamoto, T.; Homma, Y. Adsorption effects on radial breathing mode of single-walled carbon nanotubes. Physical Review B 2015, 91, 155415.

2. Wilder, J. W. G.; Venema, L. C.; Rinzler, A. G.; Smalley, R. E.; Dekker, C. Electronic structure of atomically resolved carbon nanotubes. Nature 1998, 391, 59-62.

3. Li, J.; Ke, C.-T.; Liu, K.; Li, P.; Liang, S.; Finkelstein, G.; Wang, F.; Liu, J. Importance of Diameter Control on Selective Synthesis of Semiconducting Single-Walled Carbon Nanotubes. ACS Nano 2014, 8, 8564-8572.

4. Ding, F.; Larsson, P.; Larsson, J. A.; Ahuja, R.; Duan, H.; Rosén, A.; Bolton, K. The Importance of Strong Carbon−Metal Adhesion for Catalytic Nucleation of Single-Walled Carbon Nanotubes. Nano Letters 2008, 8, 463-468.

5. Ayre, G. N.; Uchino, T.; Mazumder, B.; Hector, A. L.; Hutchison, J. L.; Smith, D. C.; Ashburn, P.; Groot, C. H. d. On the mechanism of carbon nanotube formation: the role of the catalyst. Journal of Physics: Condensed Matter 2011, 23, 394201.

6. Li, X.; Tu, X.; Zaric, S.; Welsher, K.; Seo, W. S.; Zhao, W.; Dai, H. Selective synthesis combined with chemical separation of single-walled carbon nanotubes for chirality selection. Journal of the American Chemical Society 2007, 129, 15770-15771.

7. Krupke, R.; Hennrich, F.; Löhneysen, H. v.; Kappes, M. M. Separation of Metallic from Semiconducting Single-Walled Carbon Nanotubes. Science 2003, 301, 344-347.

8. Ghosh, S.; Bachilo, S. M.; Weisman, R. B. Advanced sorting of single-walled carbon nanotubes by nonlinear density-gradient ultracentrifugation. Nat Nano 2010, 5, 443-450.

9. Chen, Z.; Du, X.; Du, M.-H.; Rancken, C. D.; Cheng, H.-P.; Rinzler, A. G. Bulk Separative Enrichment in Metallic or Semiconducting Single-Walled Carbon Nanotubes. Nano Letters 2003, 3, 1245-1249.

10. Strano, M. S.; Dyke, C. A.; Usrey, M. L.; Barone, P. W.; Allen, M. J.; Shan, H.; Kittrell, C.; Hauge, R. H.; Tour, J. M.; Smalley, R. E. Electronic Structure Control of Single-Walled Carbon Nanotube Functionalization. Science 2003, 301, 1519-1522.

11. Voggu, R.; Rao, K. V.; George, S. J.; Rao, C. N. R. A Simple Method of Separating Metallic and Semiconducting Single-Walled Carbon Nanotubes Based on Molecular Charge Transfer. Journal of the American Chemical Society 2010, 132, 5560-5561.

12. Cheung, C. L.; Kurtz, A.; Park, H.; Lieber, C. M. Diameter-Controlled Synthesis of Carbon Nanotubes. The Journal of Physical Chemistry B 2002, 106, 2429-2433.

13. Nasibulin, A. G.; Pikhitsa, P. V.; Jiang, H.; Kauppinen, E. I. Correlation between catalyst particle and single-walled carbon nanotube diameters. Carbon 2005, 43, 2251-2257.

14. Saito, T.; Ohmori, S.; Shukla, B.; Yumura, M.; Iijima, S. A Novel Method for Characterizing the Diameter of Single-Wall Carbon Nanotubes by Optical Absorption Spectra. Applied Physics Express 2009, 2, 095006-095006-095003.

15. Tian, Y.; Timmermans, M. Y.; Kivistö, S.; Nasibulin, A. G.; Zhu, Z.; Jiang, H.; Okhotnikov, O. G.; Kauppinen, E. I. Tailoring the diameter of single-walled carbon nanotubes for optical applications. Nano Research 2011, 4, 807-815.

16. Hedman, D.; Reza Barzegar, H.; Rosén, A.; Wågberg, T.; Andreas Larsson, J. On the Stability and Abundance of Single Walled Carbon Nanotubes. Scientific Reports 2015, 5, 16850.

17. Lukas, D.; Jason, G.; Thomas, H.; Matthias, M.; Roland, R.; Christofer, H. Narrowing SWNT diameter distribution using size-separated ferritin-based Fe catalysts. Nanotechnology 2009, 20, 355601.

18. Dai, H.; Rinzler, A. G.; Nikolaev, P.; Thess, A.; Colbert, D. T.; Smalley, R. E. Single-wall nanotubes produced by metal-catalyzed disproportionation of carbon monoxide. Chemical Physics Letters 1996, 260, 471-475.

19. Kukovitsky, E. F.; L'Vov, S. G.; Sainov, N. A.; Shustov, V. A.; Chernozatonskii, L. A. Correlation between metal catalyst particle size and carbon nanotube growth. Chemical Physics Letters 2002, 355, 497-503.

20. Chen, G.; Seki, Y.; Kimura, H.; Sakurai, S.; Yumura, M.; Hata, K.; Futaba, D. N. Diameter control of single-walled carbon nanotube forests from 1.3–3.0 nm by arc plasma deposition. Scientific Reports 2014, 4, 3804.

21. Mattevi, C.; Wirth, C. T.; Hofmann, S.; Blume, R.; Cantoro, M.; Ducati, C.; Cepek, C.; Knop-Gericke, A.; Milne, S.; Castellarin-Cudia, C.; Dolafi, S.; Goldoni, A.; Schloegl, R.; Robertson, J. In-situ X-ray Photoelectron Spectroscopy Study of Catalyst−Support Interactions and Growth of Carbon Nanotube Forests. The Journal of Physical Chemistry C 2008, 112, 12207-12213.

22. Kim, S. M.; Pint, C. L.; Amama, P. B.; Zakharov, D. N.; Hauge, R. H.; Maruyama, B.; Stach, E. A. Evolution in Catalyst Morphology Leads to Carbon Nanotube Growth Termination. The Journal of Physical Chemistry Letters 2010, 1, 918-922.

23. Yao, Y.; Feng, C.; Zhang, J.; Liu, Z. "Cloning" of Single-Walled Carbon Nanotubes via Open-End Growth Mechanism. Nano Letters 2009, 9, 1673-1677.

24. Liu, B.; Liu, J.; Tu, X.; Zhang, J.; Zheng, M.; Zhou, C. Chirality-Dependent Vapor-Phase Epitaxial Growth and Termination of Single-Wall Carbon Nanotubes. Nano Letters 2013, 13, 4416-4421.

25. Liu, J.; Wang, C.; Tu, X.; Liu, B.; Chen, L.; Zheng, M.; Zhou, C. Chirality-controlled synthesis of single-wall carbon nanotubes using vapour-phase epitaxy. Nat Commun 2012, 3, 1199.

26. Almkhelfe, H.; Carpena-Núñez, J.; Back, T. C.; Amama, P. B. Gaseous product mixture from Fischer–Tropsch synthesis as an efficient carbon feedstock for low temperature CVD growth of carbon nanotube carpets. Nanoscale 2016, 8, 13476-13487.

27. Almkhelfe, H.; Li, X.; Rao, R.; Amama, P. B. Catalytic CVD growth of millimeter-tall single-wall carbon nanotube carpets using industrial gaseous waste as a feedstock. Carbon 2017, 116, 181-190.

28. Kharlamova, M. V. Investigation of growth dynamics of carbon nanotubes. Beilstein journal of nanotechnology 2017, 8, 826.

29. Sakurai, S.; Nishino, H.; Futaba, D. N.; Yasuda, S.; Yamada, T.; Maigne, A.; Matsuo, Y.; Nakamura, E.; Yumura, M.; Hata, K. Role of Subsurface Diffusion and Ostwald Ripening in Catalyst Formation for Single-Walled Carbon Nanotube Forest Growth. Journal of the American Chemical Society 2012, 134, 2148-2153.

30. Yang, N.; Li, M.; Patscheider, J.; Youn, S. K.; Park, H. G. A Forest of Sub-1.5-nm-wide Single-Walled Carbon Nanotubes over an Engineered Alumina Support. 2017, 7, 46725.

31. Amama, P. B.; Pint, C. L.; McJilton, L.; Kim, S. M.; Stach, E. A.; Murray, P. T.; Hauge, R. H.; Maruyama, B. Role of Water in Super Growth of Single-Walled Carbon Nanotube Carpets. Nano Letters 2009, 9, 44-49.

32. Liu, B.; Ren, W.; Li, S.; Liu, C.; Cheng, H.-M. High temperature selective growth of single-walled carbon nanotubes with a narrow chirality distribution from a CoPt bimetallic catalyst. Chemical Communications 2012, 48, 2409-2411.

33. Kiang, C.-H. Growth of large-diameter single-walled carbon nanotubes. The Journal of Physical Chemistry A 2000, 104, 2454-2456.

34. An, H.; Kumamoto, A.; Takezaki, H.; Ohyama, S.; Qian, Y.; Inoue, T.; Ikuhara, Y.; Chiashi, S.; Xiang, R.; Maruyama, S. Chirality specific and spatially uniform synthesis of single-walled carbon nanotubes from a sputtered Co-W bimetallic catalyst. Nanoscale 2016, 8, 14523-14529.

35. Gomez-Ballesteros, J. L.; Balbuena, P. B. Structure and dynamics of metallic and carburized catalytic Ni nanoparticles: effects on growth of single-walled carbon nanotubes. Physical Chemistry Chemical Physics 2015, 17, 15056-15064.

36. Maultzsch, J.; Telg, H.; Reich, S.; Thomsen, C. Radial breathing mode of single-walled carbon nanotubes: Optical transition energies and chiral-index assignment. Physical Review B 2005, 72, 205438.